



Quantifying the role of antiferromagnetic fluctuations in the superconductivity of the doped Hubbard model

Xinyang Dong¹, Emanuel Gull¹ and Andrew J. Millis¹ Andrew J. Millis 1 Andrew J. Millis 2 Andrew J. Mi

Superconductivity arises from the pairing of charge-e electrons into charge-2e bosons—called Cooper pairs—and their condensation into a coherent quantum state. The exact mechanism by which electrons pair up into Cooper pairs in high-temperature superconductors is still not understood. One of the plausible candidates is that spin fluctuations can provide an attractive effective interaction that enables this 1-3. Here we study the contribution of the electron-spin-fluctuation coupling to the superconducting state of the two-dimensional Hubbard model within dynamical cluster approximation4 using a numerically exact continuous-time Monte Carlo solver5. We show that only about half of the superconductivity can be attributed to a pairing mechanism arising from treating spin fluctuations as a pairing boson in the standard one-loop theory. The rest of the pairing interaction must come from as-yet unidentified higher-energy processes.

In conventional superconductors such as lead, a comparison of the frequency dependence of the superconducting gap function to the frequency spectrum of phonons (quantized lattice vibrations)^{6,7} establishes the fact that the electron–phonon interaction provides the pairing glue that binds electrons into Cooper pairs. Many unconventional superconductors are now known⁸⁻¹¹ in which the pairing glue is believed not to be provided by phonons. Substantial indirect evidence indicates that in many cases, the relevant interaction is the exchange of spin fluctuations¹⁻³, but direct evidence has been lacking and many other mechanisms have been proposed¹²⁻¹⁷.

The theoretical study of unconventional superconductivity that is believed to arise from strong electron–electron interactions requires a model that captures the essentials of correlated electron physics, and can be studied non-perturbatively. The Hubbard model 18,19 has been proposed as the minimal theoretical model of quantum materials such as the copper-oxide-based high- T_c (T_c , transition temperature) superconductors²⁰. This model describes electron hopping among sites of a lattice (here we consider the two-dimensional square lattice case with nearest-neighbour hopping of amplitude t) and subject to a site-local repulsive interaction U.

To have non-perturbative access to both static phase diagram and dynamical properties, we use the dynamical cluster approximation (DCA)⁴ method. In DCA, the electron propagator and spin-fluctuation spectrum are computed within the same formalism and at the same level of approximation, enabling a quantitative analysis of the electron–spin-fluctuation interaction. The resulting solution^{21,22} produces a good qualitative description of the physics of the high- T_c copper oxide superconductors, including a high-doping Fermi-liquid regime, a Mott insulator, a low-doping pseudogap

and an intermediate-doping dome of d-wave superconductivity. The extent to which a stripe magnetic phase pre-empts the superconducting phase found in the DCA is currently under debate^{19,23}, but we emphasize that the superconductivity found in DCA is well defined and locally stable, with properties that we study in this paper.

We quantify the strength of the electron–spin-fluctuation coupling in the model by analysing the frequency dependence of the computationally determined electron self-energy, superconducting gap function and spin-fluctuation spectrum. Our analysis shows that at intermediate interaction and slightly overdoped regime, about half of the superconductivity is attributable to spin fluctuations in the one-loop spin fluctuation theory, with the other half coming from higher-energy processes.

We investigated several different doping levels and interaction strengths. We present here the results obtained for doping $x\approx 0.10$ (carrier concentration n=1-x per site) and temperatures as low as T=t/50. For this carrier concentration at U=6t, the normal state is a momentum-space-differentiated Fermi liquid outside the pseudogap regime, corresponding to the overdoped side of the cuprates. The superconducting state, which we explicitly construct, appears below $T_c\approx t/40$. The choice of parameters is influenced by the following considerations: for higher U, calculations become more difficult⁵, whereas for lower U, they are less relevant for strong correlation superconductivity. Higher doping levels reduce T_c , whereas lower doping levels enhance the effects of the nearby pseudogap and the effects of the antiferromagnetic state around half-filling, making one-loop spin-fluctuation theory less likely to succeed. We will briefly comment on the results for different doping levels in the conclusions.

We calculate the normal (N) and anomalous (A) components of the electron self-energy. Using recent algorithmic developments²⁴, we also calculated the impurity-model spin susceptibilities χ in both normal and superconducting states.

Spin-fluctuation theories yield the contribution of spin fluctuation (SF) to the N and A self-energies in terms of spin susceptibility as well as N and A components of the Green function $G_K^{N/A}$ as 1,3,6,25 (Fig. 1)

$$\Sigma_K^{\text{SF;N/A}}(\omega) = g^2 \frac{1}{\beta N} \sum_{\Omega, \Omega} \chi_Q(\Omega) G_{K-Q}^{N/A}(\omega - \Omega). \tag{1}$$

We assess the relevance of spin fluctuations by using our calculated G and χ , along with an estimated coupling constant g to compare Σ^{SF} (equation (1)) with our numerically calculated self-energies.

¹Department of Physics, University of Michigan, Ann Arbor, MI, USA. ²Center for Computational Quantum Physics, Flatiron Institute, New York, NY, USA. ³Department of Physics, Columbia University, New York, NY, USA. [∞]e-mail: egull@umich.edu; amillis@flatironinstitute.org

LETTERS NATURE PHYSICS



Fig. 1 | Spin-fluctuation diagrams for normal and anomalous self-energy. Solid lines denote normal or anomalous Green's function and wavy lines, spin susceptibility.

The method to estimate g^2 is explained in detail in Methods. In general, we partition the imaginary part of the real-frequency self-energy into a low-frequency part that we suppose arises mainly from spin fluctuations and a higher-frequency part that represents all the other processes contributing to the imaginary part of the self-energy: $\mathrm{Im} \Sigma_K^N(\omega) = \mathrm{Im} \Sigma_K^{\mathrm{SF;N}}(\omega) + \mathrm{Im} \Sigma_K^{\mathrm{high:N}}(\omega)$,. We take $\Sigma^{\mathrm{SF;N}}$ to have the functional form of equation (1) and determine g^2 by requiring consistency with our numerically computed self-energies. We have computed the self-energies in all the momentum tiles but we focus here on the self-energies corresponding to the tiles centred on the antinode points $(\pi,0)/(0,\pi)$, where the superconducting gap is the maximum and the normal component of the self-energy is the largest. We consider consistency both directly on the Matsubara axis (avoiding the ambiguities associated with analytical continuation) and on the real axis. For the imaginary-axis analysis, we note that the quantity $Z_K^N = \frac{\partial [\mathrm{Re} \Sigma_K^N(\omega)]}{\partial \omega}$ related to the normal-state mass enhancement may be estimated from the Matsubara axis results as

that the quantity $Z_K^N = \frac{\partial [\operatorname{Re}\Sigma_K^N(\omega)]}{\partial \omega}$ related to the normal-state mass enhancement may be estimated from the Matsubara axis results as $Z_K^N = \frac{\operatorname{Im}(\Sigma_K^N(i\omega_1) - \Sigma_K^N(i\omega_0))}{\omega_1 - \omega_0}$ (Fig. 2, inset) and cannot be larger than the contribution from the spin-fluctuation sector.

The top panel in Fig. 2 shows the Matsubara analysis of the normal component of the antinode self-energy and the bottom panel shows the real-axis fits. Both cases are consistent with a value of $g^2 = 3.8$, implying that about 2/3 of Z^N comes from the electronspin-fluctuation interaction.

With the spin-fluctuation spectrum and the electronspin-fluctuation coupling constant in hand, we next determine the extent to which superconductivity arises from spin fluctuations by solving the anomalous component of equation (1) and comparing the result to the numerically exact continuous-time quantum Monte Carlo solution, which gives $d_{x^2-y^2}$ -symmetry superconductivity. We begin with the equation for T_c , obtained by linearizing equation (1) in the anomalous component of self-energy. The resulting equation is a linear eigenvalue equation for eigenvector $\Sigma^{A}(i\omega_{n})$; the largest eigenvalue λ increases as temperature decreases, and T_c is the temperature at which the leading eigenvalue equals unity (equation (16)). A $d_{x^2-v^2}$ -symmetry gap yields a non-negative eigenvalue. Using our estimated $g^2 = 3.8$, we find that at temperature T = t/40, the leading eigenvalue λ is about 0.5 (Fig. 3, inset); therefore, increasing the net pairing strength by a factor of about two would be needed to bring the leading eigenvalue up to 1.0 (in fact, a larger increase would be required because the coupling constant of the normal-state self-energy means that T_c does not vary linearly with the coupling).

Figure 3 compares the quantum Monte Carlo anomalous self-energy with the spin-fluctuation self-energy $\Sigma_K^{\text{SF};A}$ at $K\!=\!(0,\pi)$. We note that the spin-fluctuation interaction has two components, one from fluctuations near the antiferromagnetic wavevector (π,π) and one from fluctuations at small momenta near $Q\!=\!(0,0)$. The small momentum fluctuations make a negative contribution to Σ_K^A . At the lowest Matsubara frequency, the $\Sigma_K^{\text{SF};A}$ produced by the spin-fluctuation theory is approximately half the quantum Monte Carlo self-energy, again indicating that spin-fluctuation theory alone cannot account for the superconductivity.

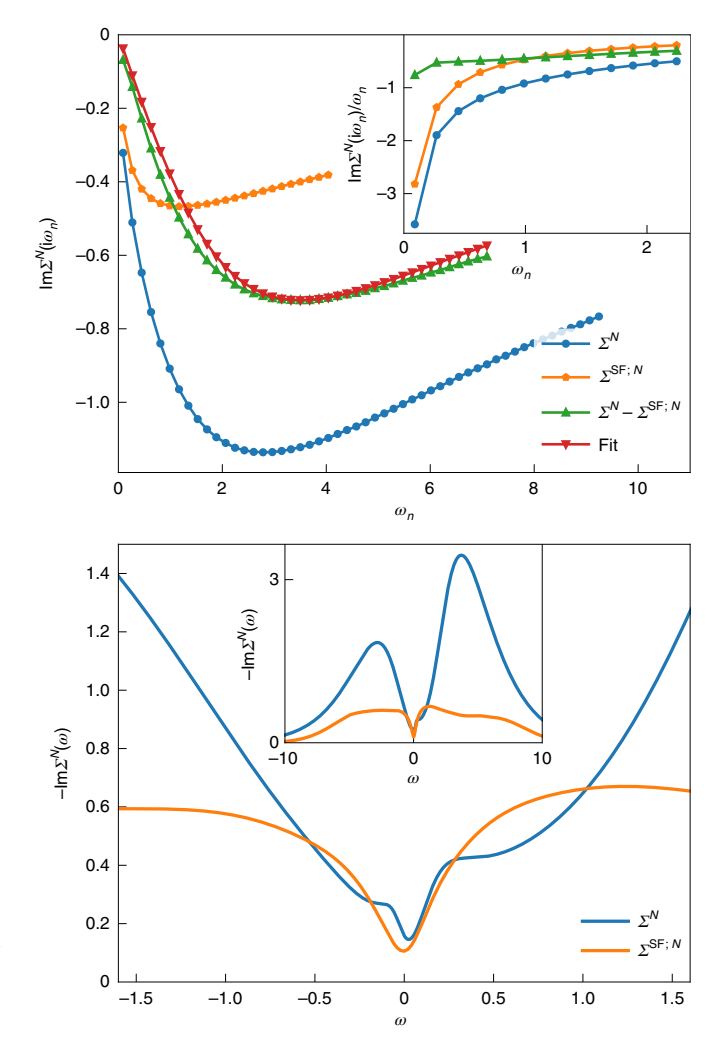


Fig. 2 | Self-energies. Imaginary part of the normal component of the Matsubara self-energy for the antinode $(0,\pi)$ at U=6.0t, $\beta t=35$ and $\mu=-1.0t$ ($n\approx0.90$) compared with spin-fluctuation self-energy computed with $g^2=3.8$ (top). The inset shows $\mathrm{Im} \Sigma_K^N(\mathrm{i}\omega_n)/\omega_n$. Negative of the analytically continued real axis, the antinode $(0,\pi)$ self-energy and spin-fluctuation contribution computed with $g^2=3.8$ (bottom). The inset shows the self-energy over a wide frequency range.

In Fig. 4, we examine the frequency dependence of gap function $\Delta(\omega)$, a complex function of real frequency defined in terms of the normal and anomalous self-energies at $K = (0, \pi)$ as 26,27

$$\Delta(\omega) = \Sigma_K^A(\omega) / \left[1 - \frac{\Sigma_K^N(\omega) - \Sigma_K^N(-\omega)}{2\omega} \right]. \tag{2}$$

Following another study⁶, we compare the frequency dependence of the spin-fluctuation spectrum, imaginary part of the DCA-computed gap function and estimated gap function computed by solving equation (1) using the continuous-time quantum Monte Carlo–computed Σ^A and χ . The real-frequency quantities are obtained from the maximum-entropy analytical continuation of the imaginary-frequency data obtained at T=t/50, well below the superconducting T_c . As noted elsewhere⁶, the presence of a gap in the electron Green function means that a peak in χ at frequency $\omega_{\rm peak}$ implies a peak in Δ at $\Delta_0 + \omega_{\rm peak}$; therefore, we shift χ by the zero-frequency gap function in the comparison.

We emphasize that the uncertainties in the analytical continuation are not small; although the areas are reliably estimated, the

NATURE PHYSICS LETTERS

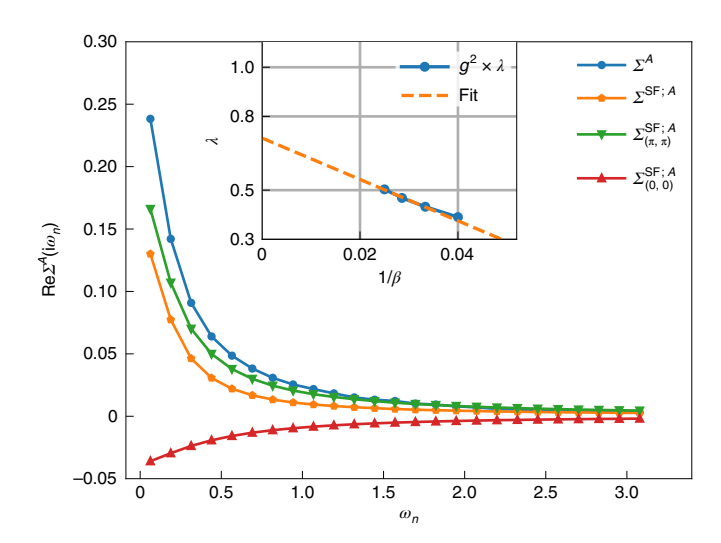


Fig. 3 | Total measured anomalous self-energy \varSigma_K^A and estimated spin-fluctuation contribution $\varSigma_K^{SF,A}$ of $K = (0,\pi)$ at U = 6.0t, $\beta t = 50$ and $\mu = -1.0t$ ($n \approx 0.90$). Individual contributions to $\varSigma^{SF,A}$ from transferred momenta $Q = (\pi,\pi)$ and Q = (0,0). The inset shows the leading eigenvalues computed from the linearized self-energy equation (equation (16)). The value of g^2 is chosen to be 3.8 for all the temperatures. The dotted line shows the linear fit to $\beta t = 30,35,40$.

peak heights and widths are subject to some uncertainty. From Fig. 4, it is evident that although the peaks in the gap function and shifted χ roughly coincide, the spin-fluctuation contribution to the imaginary part of the gap function is concentrated at lower frequencies, decaying much more rapidly than the DCA-computed gap function, further demonstrating the importance of a high-frequency non-spin-fluctuation contribution to the electron self-energy.

Spin-fluctuation theories, in which spin fluctuations (as parametrized by susceptibility) are treated as a pairing boson within the one-loop approximation, are widely considered to be promising candidates for theories of superconductivity. Here we have performed a quantitative study, in a well-defined numerically controlled theory, of the extent to which this is actually the case. The theory produces a superconducting state and a spin-fluctuation spectrum, which (taking advantage of recent developments²⁴) we can exactly obtain numerically. Access to the spin-fluctuation spectrum enables us to compare the spin-fluctuation theory calculation of the normal-state self-energies with the numerically exact results for the same quantities, thereby allowing an estimate of the electron-spin-fluctuation coupling constant. Knowledge of the coupling constant then enables a quantitative analysis of the contribution of spin fluctuations to the superconducting T_c and to the magnitude and form of the superconducting gap function. In qualitative consistency with previous results³, we find that low-frequency spin fluctuations contribute to the superconductivity, but we find that quantitatively only about half of the pairing can be attributed to these fluctuations. The other half of the pairing, therefore, arises from higher-frequency fluctuations, whose nature and precise physical origin remain to be determined.

We have similarly examined other doping values and interaction strengths (Supplementary Information). For $(U=6.0t, \mu=-0.9t (x\approx 0.089))$, $(U=6.0t, \mu=-1.1t (x\approx 0.120))$ and $(U=5.5t, \mu=-0.6t (x\approx 0.067))$, our analysis is internally consistent and provides reasonable estimates of the spin-fluctuation contribution to the self-energy. We find that as doping decreases below $x\approx 0.10$ at U=6t, spin-fluctuation theory rapidly becomes a much less satisfactory description of the normal state, with the spin-fluctuation

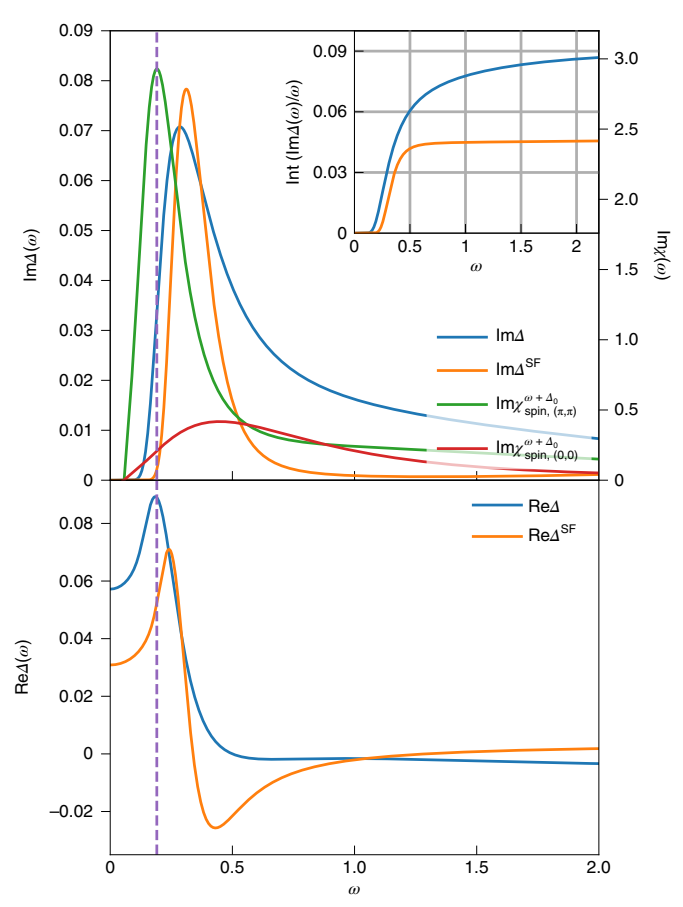


Fig. 4 | Comparison of true gap function, gap function from spin fluctuation, antiferromagnetic susceptibility ${\rm Im}\chi_{{\rm spin},(\pi,\pi)}^{\omega+\Delta_0}$ and FM susceptibility ${\rm Im}\chi_{{\rm spin},(0,0)}^{\omega+\Delta_0}$ shifted by $\Delta_0={\rm Re}\Delta(\omega=0)=0.057$ at U=6.0t, $\beta t=50$ and $\mu=-1.0$ t ($n\approx0.90$). Imaginary part (top). The inset shows the integral of ${\rm Im}\Delta(\omega)/\omega$ starting from $\omega=0$. Real part (bottom).

contribution to Σ^N apparently decreasing as T_c weakly increases. As the doping increases above $x \approx 0.10$, the spin-fluctuation contribution to the normal-state self-energy and gap function becomes larger, but T_c rapidly decreases. These results are consistent with our finding that spin fluctuations do not fully account for the superconductivity exhibited by the model. An interesting question for future research is to extend this analysis to compute the t' and U dependence of the spin-fluctuation spectrum and compare the results with the known²⁴ dependence of superconducting T_c .

The theoretical model used in this work is the eight-site cluster dynamical mean-field approximation in the 'DCA' implementation. The cluster size is chosen based on previous literature to capture the pairing and magnetic fluctuations at reasonable computational expense. Cluster dynamical mean-field theory does not adequately capture, for example, stripe physics 19,23,28-30, which may pre-empt superconductivity in some parameter ranges, and the cluster sizes available, whereas large enough to provide results that compare well with the experiment and more exact calculations, as well as cannot capture many of the interesting specifics of superconducting phenomenology. However, it is important to emphasize that the method provides a single internally consistent computational scheme that produces a well-defined locally stable superc onducting phase whose properties can be studied, and that provides—at the same level of approximation—normal and anomalous self-energies and spin-fluctuation spectra, enabling a theoretically meaningful comparison.

LETTERS NATURE PHYSICS

Our finding that spin fluctuations, as parametrized by the spin-spin correlation function χ , and coupled to electrons via the standard one-loop approximation, are not the dominant form of superconductivity suggests more generally that spin-fluctuation theories of this type may miss important aspects of correlated electron superconductivity. One may put the question in more general terms: Fig. 2 shows that an effective low-energy theory involving spin fluctuations coupled to Green's functions renormalized by high-energy processes accounts at least approximately for the normal-state self-energy. How should the low-energy theory be extended to account for the superconductivity? One may simply supplement the low-energy theory with an additional Bardeen-Cooper-Schrieffer-type pairing interaction. The frequency dependence of the gap function (Fig. 4) indicates that the microscopic physics involves a frequency scale at about t rather lower than the approximate 2-3t-frequency scale characterizing the high-energy part of the normal component of self-energy. If the nature of these higher-frequency contributions to the pairing could be elucidated, tuning the relevant degrees of freedom might be an effective strategy for raising T_c .

Online content

Any methods, additional references, Nature Research reporting summaries, source data, extended data, supplementary information, acknowledgements, peer review information; details of author contributions and competing interests; and statements of data and code availability are available at https://doi.org/10.1038/s41567-022-01710-z.

Received: 10 November 2021; Accepted: 7 July 2022; Published online: 18 August 2022

References

- Miyake, K., Schmitt-Rink, S. & C. M., Varma Spin-fluctuation-mediated even-parity pairing in heavy-fermion superconductors. *Phys. Rev. B* 34, 6554–6556 (1986).
- D. J., Scalapino Superconductivity and spin fluctuations. J. Low Temp. Phys. 117, 179–188 (1999).
- T. A., Maier, Poilblanc, D. & D. J., Scalapino Dynamics of the pairing interaction in the Hubbard and t–J models of high-temperature superconductors. *Phys. Rev. Lett.* 100, 237001 (2008).
- Maier, T., Jarrell, M., Pruschke, T. & M. H., Hettler Quantum cluster theories. Rev. Mod. Phys. 77, 1027–1080 (2005).
- Gull, E., Werner, P., Parcollet, O. & Troyer, M. Continuous-time auxiliary-field Monte Carlo for quantum impurity models. EPL 82, 57003 (2008).
- D. J., Scalapino, J. R., Schrieffer & J. W., Wilkins Strong-coupling superconductivity. I. Phys. Rev. 148, 263–279 (1966).
- W. L., McMillan Transition temperature of strong-coupled superconductors. Phys. Rev. 167, 331–344 (1968).
- Steglich, F. et al. Superconductivity in the presence of strong Pauli paramagnetism: CeCu₂Si₂. Phys. Rev. Lett. 43, 1892–1896 (1979).
- J. G., Bednorz & K. A., Müller Possible high T_c superconductivity in the Ba-La-Cu-O system. Z. Physik B—Condens. Matter 64, 189–193 (1986).
- Maeno, Y. et al. Superconductivity in a layered perovskite without copper. Nature 372, 532–534 (1994).

- Kamihara, Y. et al. Iron-based layered superconductor: LaOFeP. J. Am. Chem. Soc. 128, 10012–10013 (2006).
- Castellani, C., Di Castro, C. & Grilli, M. Non-Fermi-liquid behavior and d-wave superconductivity near the charge-density-wave quantum critical point. Z. Physik B—Condens. Matter 103, 137–144 (1996).
- C. M., Varma Non-Fermi-liquid states and pairing instability of a general model of copper oxide metals. *Phys. Rev. B* 55, 14554–14580 (1997).
- Capone, M., Fabrizio, M., Castellani, C. & Tosatti, E. Strongly correlated superconductivity and pseudogap phase near a multiband Mott insulator. *Phys. Rev. Lett.* 93, 047001 (2004).
- P. W., Anderson Is there glue in cuprate superconductors? Science 316, 1705–1707 (2007).
- T. D., Stanescu, Galitski, V. & Das Sarma, S. Orbital fluctuation mechanism for superconductivity in iron-based compounds. *Phys. Rev. B* 78, 195114 (2008).
- Saito, T., Yamakawa, Y., Onari, S. & Kontani, H. Revisiting orbital-fluctuation-mediated superconductivity in LiFeAs: nontrivial spin-orbit interaction effects on the band structure and superconducting gap function. *Phys. Rev. B* 92, 134522 (2015).
- J. P. F., LeBlanc et al. Solutions of the two-dimensional Hubbard model: benchmarks and results from a wide range of numerical algorithms. *Phys. Rev. X* 5, 041041 (2015).
- B.-X., Zheng et al. Stripe order in the underdoped region of the two-dimensional Hubbard model. Science 358, 1155–1160 (2017).
- P. W., Anderson The resonating valence bond state in La₂CuO₄ and superconductivity. Science 235, 1196–1198 (1987).
- Gull, E., Ferrero, M., Parcollet, O., Georges, A. & A. J., M. Momentum-space anisotropy and pseudogaps: a comparative cluster dynamical mean-field analysis of the doping-driven metal-insulator transition in the two-dimensional Hubbard model. *Phys. Rev. B* 82, 155101 (2010).
- Gull, E., Parcollet, O. & A. J., Millis Superconductivity and the pseudogap in the two-dimensional Hubbard model. *Phys. Rev. Lett.* 110, 216405 (2013).
- 23. Qin, M. et al. Absence of superconductivity in the pure two-dimensional Hubbard model. *Phys. Rev. X* **10**, 031016 (2020).
- Chen, X., J. P. F., LeBlanc & Gull, E. Superconducting fluctuations in the normal state of the two-dimensional Hubbard model. *Phys. Rev. Lett.* 115, 116402 (2015).
- P. W., Anderson & W. F., Brinkman Anisotropic superfluidity in ³He: a possible interpretation of its stability as a spin-fluctuation effect. *Phys. Rev. Lett.* 30, 1108–1111 (1973).
- 26. Poilblanc, D. & D. J., Scalapino Calculation of $\Delta(k,\omega)$ for a two-dimensional t-J cluster. *Phys. Rev. B* **66**, 052513 (2002).
- Gull, E. & A. J., Millis Pairing glue in the two-dimensional Hubbard model. Phys. Rev. B 90, 041110 (2014).
- E. W., Huang, C. B., Mendl, H.-C., Jiang, Moritz, B. & T. P., Devereaux Stripe order from the perspective of the Hubbard model. npj Quantum Mater. 3, 22 (2018)
- Wietek, A., Y.-Y., He, S. R., White, Georges, A. & E. M., Stoudenmire Stripes, antiferromagnetism, and the pseudogap in the doped Hubbard model at finite temperature. *Phys. Rev. X* 11, 031007 (2021).
- Mai, P., Karakuzu, S., Balduzzi, G., Johnston, S. & T. A., Maier Intertwined spin, charge, and pair correlations in the two-dimensional Hubbard model in the thermodynamic limit. *Proc. Natl Acad. Sci. USA* 119, e2112806119 (2022).

Publisher's note Springer Nature remains neutral with regard to jurisdictional claims in published maps and institutional affiliations.

Springer Nature or its licensor holds exclusive rights to this article under a publishing agreement with the author(s) or other rightsholder(s); author self-archiving of the accepted manuscript version of this article is solely governed by the terms of such publishing agreement and applicable law.

© The Author(s), under exclusive licence to Springer Nature Limited 2022

NATURE PHYSICS

(5)

Methods

Hubbard model, self-energy and spin susceptibility. We study the twodimensional single-band Hubbard model in both normal and superconducting states:

$$H = \sum_{k\sigma} (\epsilon_k - \mu) c_{k\sigma}^{\dagger} c_{k\sigma} + U \sum_{i} n_{i\uparrow} n_{i\downarrow}, \tag{3}$$

where μ is the chemical potential and $\varepsilon_k = -2t(\cos k_x + \cos k_y)$ is the dispersion with nearest-neighbour hopping t; U is the strength of the interaction, i labels a lattice site, *k* labels the momentum and *n* is the density operator.

We measure Green's function matrix $\underline{G}(k, i\omega_n)$ in the impurity solver, and the self-energy can be computed from the Dyson equation

$$\Sigma(k, i\omega_n) = G_0^{-1}(k, i\omega_n) - G^{-1}(k, i\omega_n), \tag{4}$$

where

$$\underline{G}(k,\tau) = -\langle \mathcal{T} \begin{pmatrix} c_{k\uparrow}(\tau)c_{k\uparrow}^{\dagger}(0) & c_{k\uparrow}(\tau)c_{-k\downarrow}(0) \\ c_{-k\downarrow}^{\dagger}(\tau)c_{k\uparrow}^{\dagger}(0) & c_{-k\downarrow}^{\dagger}(\tau)c_{-k\downarrow}(0) \end{pmatrix} \rangle,$$

$$\begin{split} \underline{G}(k, \mathrm{i}\omega_n) &= \int_0^\beta \mathrm{d}\tau \mathrm{e}^{\mathrm{i}\omega_n\tau} \underline{G}(k, \tau) \\ &= \begin{pmatrix} G_{k\uparrow}^N(\mathrm{i}\omega_n) & G_{k\uparrow}^A(\mathrm{i}\omega_n) \\ G_{k\uparrow}^{A*}(\mathrm{i}\omega_n) & -G_{-k\downarrow}^N(-\mathrm{i}\omega_n) \end{pmatrix}, \end{split} \tag{6}$$

$$\underline{G}_0^{-1}(k, i\omega_n) = \begin{pmatrix} i\omega_n - \epsilon_k + \mu & 0\\ 0 & i\omega_n + \epsilon_k - \mu \end{pmatrix}, \tag{7}$$

$$\underline{\Sigma}(k, i\omega_n) = \begin{pmatrix} \Sigma_{k\uparrow}^N(i\omega_n) & \Sigma_{k\uparrow}^A(i\omega_n) \\ \Sigma_{k\uparrow}^{A*}(i\omega_n) & -\Sigma_{-k\downarrow}^N(-i\omega_n) \end{pmatrix}. \tag{8}$$

The SU(2) symmetry of the system gives $G_{\uparrow}^{N} = G_{\downarrow}^{N}$.

The magnetic susceptibility is defined with the correlator of magnetization in the z direction, that is, $\hat{S}_z = n_{\uparrow} - n_{\downarrow}$:

$$\chi_{\text{spin}}(q,\tau) = \langle \mathcal{T}\hat{S}_z(q,\tau)\hat{S}_z(-q,0)\rangle - \langle \hat{S}_z(q)\rangle^2, \tag{9}$$

$$\chi_{\text{spin}}(q, i\Omega_n) = \int_0^\beta d\tau e^{i\Omega_n \tau} \chi_{\text{spin}}(q, \tau).$$
(10)

We measure $\chi_{\rm spin}(q, au)$ on the Chebyshev–Gauss–Lobatto collocation points and compute $\chi_{\rm spin}(q, {\rm i}\Omega_n)$ via spectral transform^{31,32}

Numerical method. We use the DCA approach to compute the single-particle Green function and susceptibility. The DCA⁴ proceeds by tiling the Brillouin zone into N equal-area non-overlapping tiles a centred at momentum points K_a and approximating the electron self-energy as $\Sigma_k(\mathrm{i}\omega_n) \to \Sigma_{K_a}(\mathrm{i}\omega_n)$ for k in tile a, so that the momentum dependence is approximated as a sum of piecewise constant functions and the full frequency dependence is retained. The $\Sigma_{K_n}(\mathrm{i}\omega_n)$ values are obtained from the solution of an N-site quantum impurity model with the same interaction *U* as in the original model and single-particle parameters obtained by a self-consistency condition. We have chosen N=8, which provides sufficient momentum resolution and allowing for calculation of the detailed dynamical information needed here.

The impurity model is solved with the continuous-time quantum Monte Carlo methods5,

Coupling constant. We compute the one-loop spin fluctuations in the Matsubara frequency space via

$$\Sigma_K^{\text{SF;N/A}}(i\omega_n) = \frac{g^2}{\beta N} \sum_{\Omega \in \Omega} \chi_Q(i\Omega_n) G_{K-Q}^{N/A}(i\omega_n - i\Omega_n). \tag{11}$$

To estimate the coupling constant g^2 , we partition the exact normal self-energy from DCA into a low-frequency part that is supposed to arise mainly from spin fluctuations and a higher-frequency part that represents contributions from all the other processes:

$$\operatorname{Im} \Sigma_{K}^{N}(i\omega_{n}) = \operatorname{Im} \Sigma_{K}^{SF;N}(i\omega_{n}) + \operatorname{Im} \Sigma_{K}^{high;N}(i\omega_{n}), \tag{12}$$

where the high-frequency process is fitted by a minimal two-parameter equation

$$\operatorname{Im} \Sigma_K^{\operatorname{fit};N}(\mathrm{i}\omega_n) = -\frac{A}{\pi} \frac{\omega_n}{\omega_n^2 + \kappa_n^2}, \tag{13}$$

with A and x_0 being two fitting parameters. The other relation we impose in the fitting procedure is that the quasi-particle weight $\left[1 - \frac{\partial [\operatorname{Re}\Sigma_{k}^{N}(\omega)]}{\partial \omega}\right]^{-1}$ given by the exact self-energy and approximated self-energy from the spin fluctuation plus the high-frequency fitting are approximately the same.

$$Z_K^N = Z_K^{\text{fit};N} + Z_K^{\text{SF};N},\tag{14a}$$

$$Z_K^N = \frac{\operatorname{Im}(\Sigma_K^N(\mathrm{i}\omega_1) - \Sigma_K^N(\mathrm{i}\omega_0))}{\omega_1 - \omega_0}.$$
 (14b)

The fitting procedure is as follows:

- For a given g^2 , compute $\Sigma_K^{\text{SF};N}(\mathrm{i}\omega_n)$ as in equation (11).
- For a given g, compute Σ_K (ido_n) as in equation (11).
 Compute Im Σ_K^{high;N}(iω_n) as in equation (12).
 Fit Im Σ_K^{fit;N}(iω_n) to Im Σ_K^{high;N}(iω_n) by computing the two fitting parameters A and x₀ from the maximum of Im Σ_K^{high;N}(iω_n).
- Compute \bar{g}^2 from the requirement of equation (14).
- The value of g^2 is decided by requiring $g^2 = \bar{g}^2$ in the above procedure, under the constraint A>0, $-\mathrm{Im}\Sigma_K^{\mathrm{SF};N}(\mathrm{i}\omega_n)\leq -\mathrm{Im}\Sigma_K^N(\mathrm{i}\omega_n)$, $\forall n$ and $-Z_K^{\mathrm{SF};N}\leq -Z_K^N$.

Linearized self-energy equation. From the matrix form of the Dyson equation, the linearized anomalous Green function can be computed as

$$G_K^A(i\omega_n) = \frac{\operatorname{Im} G_K^N(i\omega_n)}{\omega_n - \operatorname{Im} \Sigma_K^N(i\omega_n)} \Sigma_K^A(i\omega_n). \tag{15}$$

In an eight-site DCA simulation with d-wave superconductivity, the anomalous Green function and self-energy will only be non-zero at $K = (0, \pi)$ and $(\pi, 0)$, and $G^{A}_{(0,\pi)}(i\omega_n) = -G^{A}_{(\pi,0)}(i\omega_n)$ and $G^{N}_{(0,\pi)}(i\omega_n) = G^{N}_{(\pi,0)}(i\omega_n)$. The one-loop spin fluctuations (equation (11)) can then be rewritten as

$$\begin{split} \Sigma_{(0,\pi)}^{A}(\mathrm{i}\omega_{n}) \\ &= \frac{g^{2}}{\beta N} \sum_{\omega_{m}} \left[\chi_{(0,0)}(\mathrm{i}\omega_{n} - \mathrm{i}\omega_{m}) - \chi_{(\pi,\pi)}(\mathrm{i}\omega_{n} - \mathrm{i}\omega_{m}) \right] \\ &\qquad \times \frac{\mathrm{Im}G_{(0,\pi)}^{N}(\mathrm{i}\omega_{m})}{\omega_{m} - \mathrm{Im}\Sigma_{(0,\pi)}^{N}(\mathrm{i}\omega_{m})} \Sigma_{(0,\pi)}^{A}(\mathrm{i}\omega_{m}) \\ &= \sum_{\omega_{m}} F(\mathrm{i}\omega_{n}, \mathrm{i}\omega_{m}) \Sigma_{(0,\pi)}^{A}(\mathrm{i}\omega_{m}), \end{split} \tag{16}$$

where $F(i\omega_n, i\omega_m)$ is a matrix in ω_n and ω_m . The leading eigenvalue λ of this matrix should cross one at T_c , if spin fluctuations of this form cause superconductivity; otherwise, it denotes the fraction of superconductivity given by one-loop spin fluctuations.

Data availability

The datasets analysed during the current study are available via GitHub at https:// github.com/CQMP/SCgap. Simulation data are available from the corresponding authors on request.

Code availability

Computer codes for data analysis are available from the corresponding authors upon request.

References

- 31. Shen, J., Tang, T. & Wang, L.-L. Spectral Methods: Algorithms, Analysis and Applications Vol. 41 (Springer, 2011).
- 32. Gull, E., Iskakov, S., Krivenko, I., A. A., Rusakov & Zgid, D. Chebyshev polynomial representation of imaginary-time response functions. Phys. Rev. B 98, 075127 (2018).
- 33. Gull, E. et al. Continuous-time Monte Carlo methods for quantum impurity models. Rev. Mod. Phys. 83, 349-404 (2011).

Acknowledgements

X.D. is supported by NSF DMR 2001465. E.G. is supported by NSF DMR 2001465. The Flatiron Institute is a division of the Simons Foundation.

LETTERS NATURE PHYSICS

Author contributions

X.D. participated in designing the project, writing the simulation and post-processing code, running the simulations, analysing the data and writing the paper. E.G. participated in designing the project, writing the simulation code, analysing the data and writing the paper. A.J.M. participated in designing the project, analysing the data and writing the paper.

Competing interests

The authors declare no competing interests.

Additional information

Supplementary information The online version contains supplementary material available at https://doi.org/10.1038/s41567-022-01710-z.

Correspondence and requests for materials should be addressed to Emanuel Gull or Andrew J. Millis.

Peer review information *Nature Physics* thanks Yao Wang, Matthias Eschrig and Ilya Eremin for their contribution to the peer review of this work.

Reprints and permissions information is available at www.nature.com/reprints.